Ceylon Journal of Science 45(2) 2016: 71-77
DOI: http://doi.org/10.4038/cjs.v45i2.7390

RESEARCH ARTICLE

Third order perturbed energy of fcc ferromagnetic thin films as described by Heisenberg Hamiltonian

P. Samarasekara[1,3,*] and N.U.S. Yapa[2,3]

[1]*Department of Physics, University of Peradeniya, Peradeniya, Sri Lanka*
[2]*Department of Physics, Open University of Sri Lanka, Kandy, Sri Lanka*
[3]*Postgraduate Institute of Science, Peradeniya, Sri Lanka*

Received: 26 May 2016; Accepted: 06 July 2016

Abstract: Magnetic energy of fcc structured ferromagnetic thin films was investigated using third order perturbed Heisenberg Hamiltonian with seven magnetic energy parameters by a MATLAB computer program for the first time. Spin exchange interaction, magnetic dipole interaction, second order anisotropy, fourth order anisotropy, applied field, demagnetization factor and stress induced anisotropy were taken into account. Ultra-thin films with three layers (N=3) were considered. Several magnetic easy and hard directions were found in all the 3-D plots. According to some graphs, the angle between easy and hard directions was 90 degrees. Previously, the third order perturbed Heisenberg Hamiltonian with spin exchange interaction, second order magnetic anisotropy and stress induced anisotropy terms only was solved manually for ferromagnetic films with two and three layers by us. Due to the unavailability of the experimental values of these seven magnetic parameters, some reasonable values were used for this simulation.

Keywords: Heisenberg Hamiltonian, perturbation, thin films, ferromagnetic.

INTRODUCTION

Previously the Heisenberg Hamiltonian up to 2^{nd} order perturbation with few magnetic energy parameters has been solved by some other researchers. Ferromagnetic thin films have been studied using the Heisenberg Hamiltonian with spin exchange interaction, magnetic dipole interaction, applied magnetic field, second and fourth order magnetic anisotropy terms (Hucht and Usadel, 1997; Hucht and Usadel, 1999; Usadel and Hucht, 2002). Domain structure and Magnetization reversal in thin magnetic films have been theoretically investigated (Nowak, 1995). In-plane dipole coupling anisotropy of a square ferromagnetic Heisenberg monolayer has been explained using Heisenberg Hamiltonian (Dantziger *et al*., 2002). Effect of the interracial coupling on the magnetic ordering in ferro-antiferromagntic bilayers has been studied using the Heisenberg Hamiltonian (Tsai *et al*., 2003).

Due to the applications of magnetic thin films in magnetic and microwave devices, magnetic thin films are synthesized using many different techniques. Previously strontium ferrite (Hegde *et al*., 1994) and nickel ferrite (Samarasekara, 2003) films were synthesized using sputtering by us. In addition, lithium mixed ferrite films were fabricated using pulsed laser deposition (Samarasekara, 2002). For all these films, the coercivity of film increased due to the stress induced anisotropy. The change of coercivity due to the stress induced anisotropy was qualitatively calculated for all these films. The calculated values of the change of coercivity agreed with the experimentally found values. So the stress induced anisotropy plays a major role in magnetic thin fabrications. Previously the Heisenberg Hamiltonian was employed to investigate the second order perturbed energy of ultrathin ferromagnetic films (Samarasekara, 2006a), unperturbed energy of thick ferromagnetic films (Samarasekara, 2006b), unperturbed energy of spinel ferrite films (Samarasekara, 2007), second order perturbed energy of thick ferromagnetic films (Samarasekara and De Silva, 2007), third order perturbed energy of thick spinel ferrite (Samarasekara, 2011), third order perturbed energy of thin spinel ferrite (Samarasekara and Mendoza, 2011), second order perturbed energy of thick spinel ferrite films (Samarasekara, 2010)

**Corresponding Author's Email*: pubudus@pdn.ac.lk

and spin reorientation of barium ferrite (Samarasekara and Saparamadu, 2013). The magnetic dipole interaction and demagnetization factor are microscopic and macroscopic effects, respectively. Therefore, both these terms were taken into consideration in our model.

Other theoretical work of magnetic thin films can be summarized as following. EuTe films with surface elastic stresses have been theoretically studied using Heisenberg Hamiltonian (Radomska and Balcerzak, 2003). Magnetostriction of dc magnetron sputtered FeTaN thin films has been theoretically studied using the theory of De Vries (Cates and Alexander, 1994). Magnetic layers of Ni on Cu have been theoretically investigated using the Korringa-Kohn-Rostoker Green's function method (Ernst *et al*., 2000). Electric and magnetic properties of multiferroic thin films have been theoretically explained by modified Heisenberg and transverse Ising model using Green's function technique (Kovachev and Wesselinowa, 2009). The quasistatic magnetic hysteresis of ferromagnetic thin films grown on a vicinal substrate has been theoretically investigated by Monte Carlo simulations within a 2D model (Zhao *et al*., 2002). Structural and magnetic properties of two dimensional FeCo orders alloys deposited on W(110) substrates have been studied using first principles band structure theory (Spisak and Hafner, 2005).

MODEL

The Heisenberg Hamiltonian with all seven magnetic parameters can be expressed as below.

$$H= -\frac{J}{2}\sum_{m,n}\vec{S}_m.\vec{S}_n+\frac{\omega}{2}\sum_{m\neq n}\left(\frac{\vec{S}_m.\vec{S}_n}{r_{mn}^{3}}-\frac{3(\vec{S}_m.\vec{r}_{mn})(\vec{r}_{mn}.\vec{S}_n)}{r_{mn}^{5}}\right) -\sum_m D_{\lambda_m}^{(2)}(S_m^{z})^2-\sum_m D_{\lambda_m}^{(4)}(S_m^{z})^4 -\sum_{m,n}[\vec{H}-(N_d\vec{S}_n/\mu_0)].\vec{S}_m-\sum_m K_s Sin2\theta_m \quad (1)$$

Here J is spin exchange interaction, ω is the strength of long range dipole interaction, θ_m is azimuthal angle of spin, $D_{\lambda_m}^{(2)}$ and $D_{\lambda_m}^{(4)}$ are second and fourth order anisotropy constants, $\vec{H}$ is the applied magnetic field, K_s is stress induced anisotropy constant, and n and m are spin plane indices. When the stress applies normal to the film plane, the angle between mth spin and the stress is θ_m. In this 2-D model, only the x and y components of the spin are considered. N_d is the demagnetization factor changing from 0 (in film plane) to 1 (perpendicular to film plane) in SI units.

The total energy per unit spin can be deduced to the following equation.

$$E(\theta)= -\frac{1}{2}\sum_{m,n=1}^{N}[(JZ_{|m-n|}-\frac{\omega}{4}\Phi_{|m-n|})\cos(\theta_m-\theta_n)-\frac{3\omega}{4}\Phi_{|m-n|}\cos(\theta_m+\theta_n)] -\sum_{m=1}^{N}(D_m^{(2)}\cos^2\theta_m+D_m^{(4)}\cos^4\theta_m+H_{in}\sin\theta_m+H_{out}\cos\theta_m) +\sum_{m,n=1}^{N}\frac{N_d}{\mu_0}\cos(\theta_m-\theta_n)-K_s\sum_{m=1}^{N}\sin 2\theta_m \quad (2)$$

where m (or n) $Z_{|m-n|},\phi_{|m-n|},\theta_m(or\,\theta_n)$, N, H_{in} and H_{out} being indices of layers, number of nearest spin neighbors, constant arising from summation of dipole interactions, azimuthal angles of spins, total number of layers, in plane applied field and out of plane applied field, respectively.

With some perturbation, above angles θ_m and θ_n measured with film normal can be expressed in forms of $\theta_m=\theta+\varepsilon_m$ and $\theta_n=\theta+\varepsilon_n$, and above energy can be expanded up to the third order of ε as following. Here ε_m (or ε_n) is a small perturbation of the angle.

$$E(\theta)=E_0+E(\varepsilon)+E(\varepsilon^2)+E(\varepsilon^3) \quad (3)$$

Here, E_0=

$$-\frac{1}{2}\sum_{m,n=1}^{N}(JZ_{|m-n|}-\frac{\omega}{4}\Phi_{|m-n|})+\frac{3\omega}{8}\cos 2\theta\sum_{m,n=1}^{N}\Phi_{|m-n|} -\cos^2\theta\sum_{m=1}^{N}D_m^{(2)}-\cos^4\theta\sum_{m=1}^{N}D_m^{(4)} -N(H_{in}\sin\theta+H_{out}\cos\theta-\frac{N_d}{\mu_0}+K_s\sin 2\theta)$$

$$E(\varepsilon)=-\frac{3\omega}{8}\sin 2\theta\sum_{m,n=1}^{N}\Phi_{|m-n|}(\varepsilon_m+\varepsilon_n) +\sin 2\theta\sum_{m=1}^{N}D_m^{(2)}\varepsilon_m+2\cos^2\theta\sin 2\theta\sum_{m=1}^{N}D_m^{(4)}\varepsilon_m -H_{in}\cos\theta\sum_{m=1}^{N}\varepsilon_m+H_{out}\sin\theta\sum_{m=1}^{N}\varepsilon_m-2K_s\cos 2\theta\sum_{m=1}^{N}\varepsilon_m$$

$$E(\varepsilon^2)=\frac{1}{4}\sum_{m,n=1}^{N}(JZ_{|m-n|}-\frac{\omega}{4}\Phi_{|m-n|})(\varepsilon_m-\varepsilon_n)^2$$
$$-\frac{3\omega}{16}\cos2\theta\sum_{m,n=1}^{N}\Phi_{|m-n|}(\varepsilon_m+\varepsilon_n)^2$$
$$-(\sin^2\theta-\cos^2\theta)\sum_{m=1}^{N}D_m^{(2)}\varepsilon_m^{\ 2}$$
$$+2\cos^2\theta(\cos^2\theta-3\sin^2\theta)\sum_{m=1}^{N}D_m^{(4)}\varepsilon_m^{\ 2}$$
$$+\frac{H_{in}}{2}\sin\theta\sum_{m=1}^{N}\varepsilon_m^{\ 2}+\frac{H_{out}}{2}\cos\theta\sum_{m=1}^{N}\varepsilon_m^{\ 2}$$
$$-\frac{N_d}{2\mu_0}\sum_{m,n=1}^{N}(\varepsilon_m-\varepsilon_n)^2+2K_s\sin2\theta\sum_{m=1}^{N}\varepsilon_m^{\ 2}$$

$$E(\varepsilon^3)=\frac{\omega}{16}\sin2\theta\sum_{m,n=1}^{N}(\varepsilon_m+\varepsilon_n)^3\phi_{|m-n|}-\frac{4}{3}\cos\theta\sin\theta\sum_{m=1}^{N}D_m^{(2)}\varepsilon_m^{\ 3}$$
$$-4\cos\theta\sin\theta(\frac{5}{3}\cos^2\theta-\sin^2\theta)\sum_{m=1}^{N}D_m^{(4)}\varepsilon_m^{\ 3}$$
$$+\frac{H_{in}}{6}\cos\theta\sum_{m=1}^{N}\varepsilon_m^{\ 3}-\frac{H_{out}}{6}\sin\theta\sum_{m=1}^{N}\varepsilon_m^{\ 3}$$
$$+\frac{4K_s}{3}\cos2\theta\sum_{m=1}^{N}\varepsilon_m^{\ 3} \qquad (4)$$

After using the constraint $\sum_{m=1}^{N}\varepsilon_m=0$, $E(\varepsilon)=\vec{\alpha}.\vec{\varepsilon}$

Here $\vec{\alpha}(\varepsilon)=\vec{B}(\theta)\sin2\theta$ are the terms of matrices with

$$B_\lambda(\theta)=-\frac{3\omega}{4}\sum_{m=1}^{N}\Phi_{|\lambda-m|}+D_\lambda^{(2)}+2D_\lambda^{(4)}\cos^2\theta \quad (5)$$

Also $E(\varepsilon^2)=\frac{1}{2}\vec{\varepsilon}.C.\vec{\varepsilon}$ (6)

Here the elements of matrix C can be given as following,

$$C_{mn}=-(JZ_{|m-n|}-\frac{\omega}{4}\Phi_{|m-n|})-\frac{3\omega}{4}\cos2\theta\Phi_{|m-n|}+\frac{2N_d}{\mu_0}$$
$$+\delta_{mn}\{\sum_{\lambda=1}^{N}[JZ_{|m-\lambda|}-\Phi_{|m-\lambda|}(\frac{\omega}{4}+\frac{3\omega}{4}\cos2\theta)]$$
$$-2(\sin^2\theta-\cos^2\theta)D_m^{(2)}$$
$$+4\cos^2\theta(\cos^2\theta-3\sin^2\theta)D_m^{(4)}+H_{in}\sin\theta$$
$$+H_{out}\cos\theta-\frac{4N_d}{\mu_0}+4K_s\sin2\theta\} \qquad (7)$$

In addition, third order can be expressed as the

$$E(\varepsilon^3)=\varepsilon^2\beta.\vec{\varepsilon} \qquad (8)$$

Here elements of matrix β can be given as following,

$$\beta_{mn}=\frac{3\omega}{8}\sin2\theta\Phi_{|m-n|}+\delta_{mn}\{\frac{\omega}{8}\sin2\theta[A_m-\Phi_0]$$
$$-\frac{4}{3}\cos\theta\sin\theta D_m^{(2)}+\frac{H_{in}}{6}\cos\theta-\frac{H_{out}}{6}\sin\theta$$
$$-4\cos\theta\sin\theta(\frac{5}{3}\cos^2\theta-\sin^2\theta)D_m^{(4)}+\frac{4K_s}{3}\cos2\theta\} \quad (9)$$

Also $\beta_{nm}=\beta_{mn}$, implying that matrix β is symmetric.

After substituting equations (8) and (6) in equation (3), total energy can be expressed as

$$E(\theta)=E_0+\vec{\alpha}.\vec{\varepsilon}+\frac{1}{2}\vec{\varepsilon}.C.\vec{\varepsilon}+\varepsilon^2\beta.\vec{\varepsilon}$$

At the energetically favorable state, the derivative of above $E(\theta)$ with respect to ε will be zero. Using that condition, ε can be found. After substituting that ε in above equation of $E(\theta)$, following equation can be derived.

$$E(\theta)=E_0-\frac{1}{2}\vec{\alpha}.C^+.\vec{\alpha}-(C^+\alpha)^2\vec{\beta}(C^+\alpha) \qquad (10)$$

The total magnetic energy has been calculated only for three layers (N=3), and the equation has been proved under the assumption of $D_1^{(2)}=D_2^{(2)}=D_3^{(2)}$ and $D_1^{(4)}=D_2^{(4)}=D_3^{(4)}$.

Following equation has been used to calculate the elements of matrix C^+.

$$C.C^+=1-\frac{E}{N} \qquad (11)$$

Here E is the matrix with all elements given by E_{mn}=1, and C^+ is a pseudo inverse.

RESULTS AND DISCUSSION

For fcc(001) lattice Z_0=4, Z_1=4 ,Z_2=0 and $\Phi_0=9.0336, \Phi_1=1.4294$(Usadel and Hucht 2002). All the graphs are given for fcc structured ferromagnetic film with three layers (N=3). Because the experimental values of J, ω, $D_m^{(2)}$, $D_m^{(4)}$, H_{in}, H_{out}, N_d and K_s are not available, these simulations were performed for some reasonable values of the ratios between those parameters. Here J, ω, $D_m^{(2)}$, $D_m^{(4)}$, H_{in}, H_{out}, $\frac{N_d}{\mu_0}$ and K_s have the dimensions of E(θ) according to equation (2). Therefore, all the ratios $\frac{E(\theta)}{\omega}$, $\frac{K_s}{\omega}$, $\frac{H_{out}}{\omega}$, $\frac{J}{\omega}$, $\frac{H_{in}}{\omega}$, $\frac{D_m^{(2)}}{\omega}$, $\frac{D_m^{(4)}}{\omega}$ and $\frac{N_d}{\mu_0\omega}$ are dimensionless. Figure 1 shows the 3-D plot of

$\frac{E(\theta)}{\omega}$ versus θ and $\frac{K_s}{\omega}$. Easy and hard direction can be found using this 3-D plot. Easy directions can be observed at $\frac{K_s}{\omega}$ =7, 17, 27, ----etc. Two easy directions with two different energies can be seen. The values of $\frac{K_s}{\omega}$ are given only for the easy directions with smaller energies. Hard directions can be observed at $\frac{K_s}{\omega}$ =6, 16, 26. ---etc. Two hard directions with different energies can be observed. The $\frac{K_s}{\omega}$ values are given for the hard directions with higher energies. For each $\frac{K_s}{\omega}$, easy and hard directions appear at 4 and 7 radians, respectively. Stress is induced in the thin films during annealing or subsequent cooling process due to the difference between thermal expansion coefficients of the film and the substrate (Samarasekara 2002).

Figure 2 shows the 3-D plot of $\frac{E(\theta)}{\omega}$ versus θ and $\frac{H_{out}}{\omega}$. Hard directions can be seen at $\frac{H_{out}}{\omega}$ =8, 18, 28, ----etc. Easy directions can be observed at $\frac{H_{out}}{\omega}$ =2, 12, 22, -----etc. Two different easy and hard directions with different energies can be observed similar to the 3-D plot of $\frac{E(\theta)}{\omega}$ versus θ and $\frac{K_s}{\omega}$. The values of $\frac{H_{out}}{\omega}$ for easy direction with smaller energy and hard direction with higher energy are given here. For some values of $\frac{H_{out}}{\omega}$, easy and hard directions can be observed at 5.43 and 7 radians, respectively.

Figure 3 shows the 3-D plot of $\frac{E(\theta)}{\omega}$ versus θ and $\frac{N_d}{\mu_0\omega}$. Several easy and hard directions can be observed in this plot. Easy directions of magnetizations can be observed at $\frac{N_d}{\mu_0\omega}$ =1, 11, 21, ----etc. In addition to these major easy directions, some minor peaks corresponding to easy directions could be observed. Hard directions of magnetizations can be seen at $\frac{N_d}{\mu_0\omega}$ =10, 20, 30, ----etc.

Figure 4 shows the 3-D plot of $\frac{E(\theta)}{\omega}$ versus θ and $\frac{J}{\omega}$. Hard directions of magnetizations can be observed at $\frac{J}{\omega}$ =11, 21, ----etc. Easy directions appear at $\frac{J}{\omega}$ =10, 20, 30, -----etc. Easy and hard directions can be seen at 1.43 and 3 radians, respectively.

CONCLUSIONS

Values of $\frac{K_s}{\omega}$, $\frac{H_{out}}{\omega}$, $\frac{N_d}{\mu_0\omega}$ and $\frac{J}{\omega}$ corresponding to easy and hard directions of magnetization were found using the 3-D plots. According to Figure 1, easy and hard directions appear at 4 and 7 radians, respectively, for each value of $\frac{K_s}{\omega}$. According to Figure 2, easy and hard directions can be observed at 5.43 and 7 radians, respectively, for some values of $\frac{H_{out}}{\omega}$. According to Figure 4, easy and hard directions can be seen at 1.43 and 3 radians, respectively. The angle between easy and hard directions is 90 degrees according to Figures 2 and 4. In some graphs, two hard or easy directions corresponding to two different energies could be found. Although this simulation was performed for some selected values of the seven magnetic parameters, this simulation can be carried out for any values of the seven magnetic parameters.

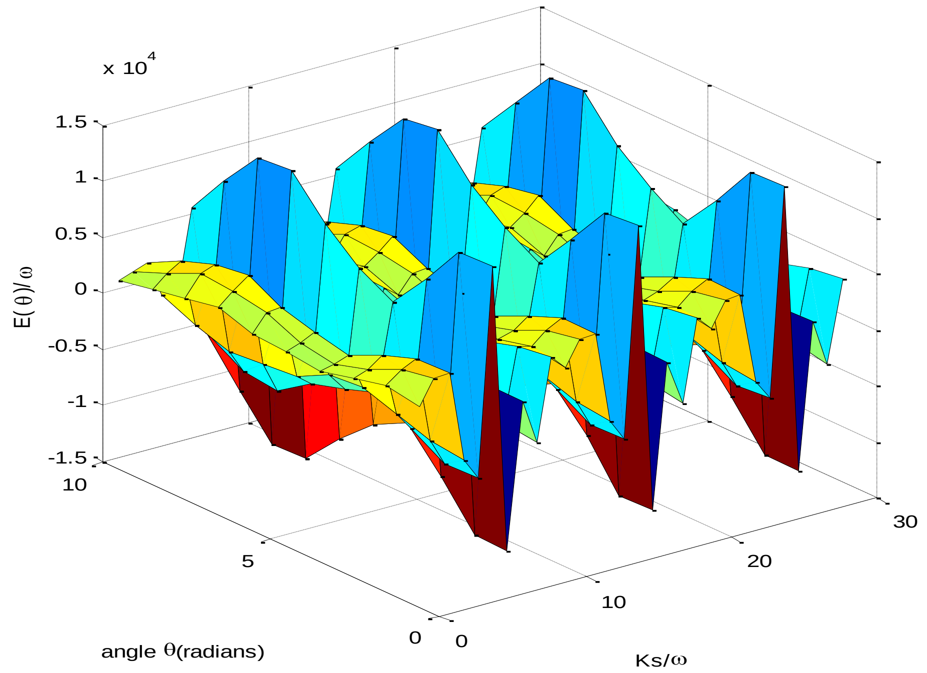

Figure 1: 3-D plot of $\dfrac{E(\theta)}{\omega}$ versus θ and $\dfrac{K_s}{\omega}$.

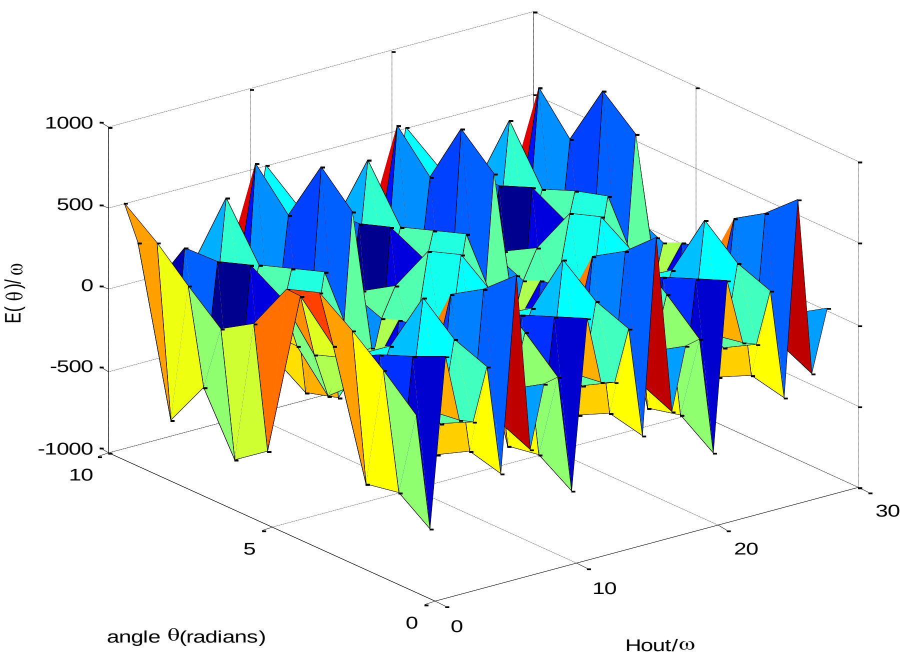

Figure 2: 3-D plot of $\dfrac{E(\theta)}{\omega}$ versus θ and $\dfrac{H_{out}}{\omega}$

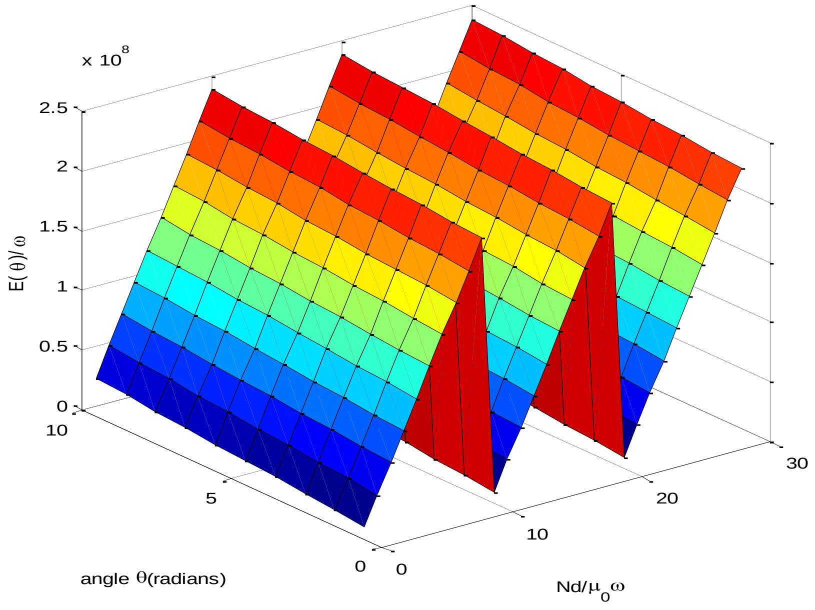

Figure 3: 3-D plot of $\frac{E(\theta)}{\omega}$ versus θ and $\frac{N_d}{\mu_0\omega}$.

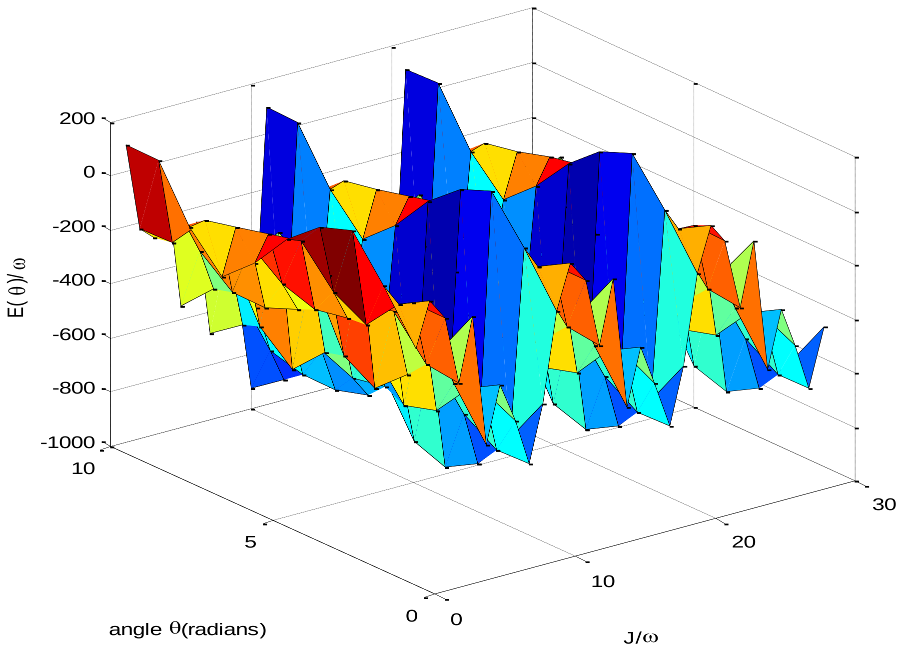

Figure 4: 3-D plot of $\frac{E(\theta)}{\omega}$ versus θ and $\frac{J}{\omega}$.

REFERENCES

Cates James C. and Alexander Jr Chester. (1994). Theoretical study of magnetostriction in FeTaN thin films. *Journal of Applied Physics* **75**: 6754-6756.

Dantziger M, Glinsmann B, Scheffler S, Zimmermann B and Jensen P.J. (2002). In-plane dipole coupling anisotropy of a square ferromagnetic Heisenberg monolayer. *Physical Review B* **66**: 094416.

Ernst A, Lueders M, Temmerman W.M, Szotek Z and Van der Laan G. (2000). Theoretical study of magnetic layers of nickel on copper; dead or live?. *Journal of Physics: Condensed matter* **12(26)**: 5599-5606.

Hegde H, Samarasekara P and Cadieu F.J. (1994). Nonepitaxial sputter synthesis of aligned strontium hexaferrites, SrO.6(Fe_2O_3), films. *Journal of Applied Physics* **75(10)**: 6640-6642.

Hucht A and Usadel K.D. (1997). Reorientation transition of ultrathin ferromagnetic films. *Physical Review B* **55**: 12309.

Hucht A and Usadel K.D. (1999). Theory of the spin reorientation transition of ultra-thin ferromagnetic films. Journal of Magnetism and Magnetic materials **203(1)**: 88-90.

Kovachev St and Wesselinowa J.M. (2009). Theoretical study of multiferroic thin films based on a microscopic model. *Journal of Physics: Condensed matter* **21(22)**: 225007.

Nowak U. (1995). Magnetisation reversal and domain structure in thin magnetic films: Theory and computer simulation. *IEEE transaction on magnetics* **31(6-2)**: 4169-4171.

Radomska Anna and Balcerzak Tadeusz (2003). Theoretical studies of model thin EuTe films with surface elastic stresses. *Central European Journal of Physics* **1(1)**: 100-117.

Samarasekara P. (2002). Easy Axis Oriented Lithium Mixed Ferrite Films Deposited by the PLD Method. *Chinese Journal of Physics* **40(6)**: 631-636.

Samarasekara P. (2003). A Pulsed RF Sputtering Method for Obtaining Higher Deposition Rates.*Chinese Journal of Physics* **41(1)**: 70-74.

Samarasekara P. (2006a). Second order perturbation of Heisenberg Hamiltonian for non- oriented ultra-thin ferromagnetic films. *Electronic Journal of Theoretical Physics* **3(11)**: 71-83.

Samarasekara P. (2006b). A solution of the Heisenberg Hamiltonian for oriented thick ferromagnetic films. *Chinese Journal of Physics* **44(5)**: 377-386.

Samarasekara P. (2007). Classical Heisenberg Hamiltonian Solution of Oriented Spinel Ferrimagnetic Thin Films. *Electronic Journal of Theoretical Physics* **4(15)**: 187-200.

Samarasekara P and De Silva S.N.P. (2007). Heisenberg Hamiltonian solution of thick ferromagnetic films with second order perturbation. *Chinese Journal of Physics* **45(2-I)**: 142-150.

Samarasekara P. (2010). Determination of energy of thick spinel ferrite films using Heisenberg Hamiltonian with second order perturbation. *Georgian electronic scientific journals: Physics* **1(3)**: 46-49.

Samarasekara P. (2011). Investigation of Third Order Perturbed Heisenberg Hamiltonian of Thick Spinel Ferrite Films. *Inventi Rapid: Algorithm Journal* **2(1)**: 1-3.

Samarasekara P and William A. Mendoza. (2011). Third Order Perturbed Heisenberg Hamiltonian of Spinel Ferrite Ultra-thin films. *Georgian electronic scientific journals: Physics* **1(5)**: 15-24.

Samarasekara P and Saparamadu Udara (2013). Easy axis orientation of barium hexa-ferrire films as explained by spin reorientation. *Georgian electronic scientific journals: Physics* **1(9)**: 10-15.

Spisak D and Hafner J. (2005). Theoretical study of FeCo/W(110) surface alloys. *Journal of Magnetism and Magnetic Materials* **286**: 386-389.

Tsai Shan-Ho, Landau D.P and Schulthess Thomas C. (2003). Effect of interracial coupling on the magnetic ordering in ferro-antiferromagntic bilayers. *Journal of Applied Physics* **93(10)**: 8612-8614.

Usadel K.D and Hucht A. (2002). Anisotropy of ultrathin ferromagnetic films and the spin reorientation transition. *Physical Review B* **66**: 024419.

Zhao D, Feng Liu, Huber D.L and Lagally M.G. (2002). Step-induced magnetic-hysteresis anisotropy in ferromagnetic thin films. *Journal of Applied Physics* **91(5)**: 3150-3153.